



Influences of Physical Parameters of a Solar Concentrator Cooker

Thierry Serge Gbembongo^{a,b*}, Auguste Mackpayen^a,
Saint-Cyr Lengaye^a and Bienvenu Pakouzou^a

^a Carnot Energy Laboratory, University of Bangui, Central African Republic.

^b Mathematics and Physics Laboratory, University of Perpignan, France.

Authors' contributions

This work was carried out in collaboration among all authors. All authors read and approved the final manuscript.

Article Information

DOI: 10.9734/JENRR/2023/v13i1255

Open Peer Review History:

This journal follows the Advanced Open Peer Review policy. Identity of the Reviewers, Editor(s) and additional Reviewers, peer review comments, different versions of the manuscript, comments of the editors, etc are available here: <https://www.sdiarticle5.com/review-history/90958>

Original Research Article

Received: 20/06/2022

Accepted: 28/08/2022

Published: 13/01/2023

ABSTRACT

This work focuses on the modelling and simulation of a solar concentrator cooker. The equations governing the heat transfers of the solar cooker are discretised by an implicit finite difference method and solved via the Gaussian algorithm, coupled with an iterative procedure. The FORTRAN numerical code that simulates the operation of the solar cooker, using meteorological data from the city of Bangui, was developed. In this simulation, the influence of physical parameters as well as of the different components of the cooker is analysed, notably: the nature of the materials used, the dimensions of the cooker. The results show that a solar flux of 900W/m² allows the determination of the different optimal parameters of the cooker. The dimensions of the parallelepipedic cooker [60 cm*50 cm*50 cm], made it possible to obtain a thermal efficiency varying from 42% to 45%. The influence of these physical parameters shows that copper is a good conductor and the thermal conductivity is higher the thinner the wall thickness (3 mm) of the pot.

Keywords: Solar cooker; physical parameters; thermal efficiency.

*Corresponding author: E-mail: gbefami2002@gmail.com;

NOMENCLATURES

R_1 and R_2	: Radius of pot (m);
e_v	: Thickness of the glass (m);
T_{ciel}	: The sky wheater ($^{\circ}\text{C}$);
m_f	: Mass of the fluid (Kg);
E_o	: Useful energy (Joules);
h_{cvai}	: Convective transfer coefficient ($\text{W}/\text{m}^2.\text{k}$);
E_i	: Energy received (Joules);
m_{ai}	: Air mass (Kg);
α_m	: Absorption coefficient (pot);
λ_v	: Thermal conductivity (vitre) ($\text{W}/\text{m}^2.\text{k}$);
h_{rv}	: Radiative transfer coefficient (glass) ($\text{W}/\text{m}^2.\text{k}$);
h_{cvv}	: Coefficient of convective transfer (glass) ($\text{W}/\text{m}^2.\text{k}$);
h_{rmv}	: Coefficient of radiative transfer of pot-glass ($\text{W}/\text{m}^2.\text{k}$);
T_{sol}	: Soil temperature ($^{\circ}\text{C}$);
S_v	: Glass area (m^2);
S_m	: Surface of the pot (m^2);
I	: Irradiation (W/m^2);
C_p	: thermal capacity ($\text{J}/\text{Kg}.\text{K}$);
h_{rmv}	: Radiative transfer coefficient ($\text{W}/\text{m}^2.\text{K}$);
∂t	: Variation of time (s);
T_{amb}	: Ambient temperature ($^{\circ}\text{C}$);
λ_m	: Thermal conductivity (pot) ($\text{W}/\text{m}^2.\text{k}$);
α_v	: Absorption coefficient of the glass;
h_f	: Coefficient of convective transfer (fluid)($\text{W}/\text{m}^2.\text{k}$);
h_{cvm}	: Coefficient of convective transfer glass-pot ($\text{W}/\text{m}^2.\text{k}$).

1. INTRODUCTION

The scarcity of fossil fuels has led the world to turn to renewable energy. Among these renewable energies, solar energy is promising and makes it possible to combat deforestation through its various applications. In the Central African Republic, the duration of sunshine is 7.6 hours per day, which favours the cooking of food using solar energy because the concentration of solar flux is one of the most promising alternatives in the current energy context for solar cookers. It is sustainable in the long term, it does not produce greenhouse gases.

Around the 1950s, the development of solar cookers became more and more significant, particularly in China and India. We are witnessing spectacular technologies, and many have designed and tested these cookers experimentally and numerically. Our study is much more focused on the numerical work that has been done on solar cookers, to predict their thermal behaviour and to see how we can study our prototype.

Thus, for parabolic trough cookers, modelling and simulation of this type of cooker is generally

carried out using MATLAB and TRNSYS.15TM software. The aim is to determine the thermal efficiency, the temperature of the heat transfer fluid at the outlet of the tube positioned at the focus of the concentrator, and the overall heat loss coefficient [1-3]. The results show that the outlet temperature of the heat transfer fluid varies from 135 to 185 $^{\circ}\text{C}$ depending on the size of the concentrator and that the thermal efficiency can reach 60.5%. For a low overall heat loss coefficient, the optical efficiency can be higher than 61%. Other works have analysed the influence of the absorber tube diameter of the solar concentrator and the tilt angle of the parabolic trough on the energy efficiency and fluid temperature at the focus of the parabolic trough [4-8]. It reveals that the water temperature can reach values above 106 $^{\circ}\text{C}$. In addition, the energy efficiency and thermal performance decrease significantly as the angle of inclination of the parabolic trough increases.

Parabolic-type cookers have been the subject of numerous numerical and experimental studies [9-18]. These numerical studies, carried out with the SIMUSOL software, are aimed at analysing the influence of solar illumination and the opening angle of the concentrator on the

temperature reached at its hearth and the cooking time of various foods (corn, rice, eggs, meat). The results show that the temperature at the focus of the concentrator can reach 150 to 300°C depending on the size of the concentrator. Furthermore, the cooking time depends on the type of food and the intensity of the solar flux. The energy efficiency reaches 60% and the cooking time of food varies from 35 to 120 minutes.

One of the purposes of the experimental work is to determine the energy efficiency of the concentrator and the temperature distributions at different points in the solar cooker [19-26]. This work is based on measurements of the temperatures of various foods (potato, chicken, macaroni) and water using type K (chromel, alumel) thermocouples with a precision of $\pm 0.5^\circ\text{C}$, type T (copper-constantan) $\pm 0.01^\circ\text{C}$. The temperature of the water in the kettle is estimated by means of a digital thermometer with a precision of $\pm 0.01^\circ\text{C}$, the global solar irradiance is measured by a solarimeter ($\pm 5\text{W}/\text{m}^2$). The measurement of temperature and relative humidity by an EKO Instruments MS-60 weather station. It has been shown that the energy efficiency reaches a maximum value of 77%, the difference between the water temperature and the ambient temperature is equal to 50°C . The water temperature varies from 95°C to 100°C at a solar irradiance of $465\text{-}1000\text{W}/\text{m}^2$.

For multi-reflector box solar cookers, the numerical work is based on the numerical solution of the transfer equations, obtained by the nodal method using MATLAB software [27-30]. The analysis of the influence of the angle of inclination of the reflector on the thermal efficiency, the temperature of the water, the absorber, the air inside the cooker and the duration of the cooking showed that, for an angle of inclination of the reflector with respect to the horizontal equal to 17° , the boiling time of 3.5 litres of water is 118 minutes and the thermal efficiency reaches 32.5%. Furthermore, the thermal efficiency and the maximum air temperature inside the cooker are equal to 33.9% and 140°C respectively.

For solar cookers with a solar heat storage unit [31-39], the phase change materials (PCMs) used were paraffin, magnesium nitrate, magnesium hexahydrate $\text{Mg}(\text{NO}_3)_2 \cdot 6\text{H}_2\text{O}$ and Lauric acid. K-type thermocouples, a digital thermometer and a Kipp&Zonen pyranometer were used to carry out various measurements.

The results show that for this type of cooker the temperature of the solar heat storage unit can vary from 120 to 165°C depending on the phase change material used. It turns out that Lauric acid is, among the PCMs used, the one that leads to the best thermal performance of the cooker. For this PCM, the energy efficiency varies from 26 to 27% for a difference between the ambient temperature and that inside the cooking chamber of 50°C .

In the light of this literature review, we conclude that box-type solar cookers are, due to their simplicity of design and construction and their ease of use, well adapted to areas without conventional energy sources. They do not present any particular disadvantage (burning). On the other hand, the concentrator type, which has a better thermal performance, has these particular disadvantages. It is for this reason that we have designed this prototype of a box-type solar cooker equipped with a solar reflector concentrator.

2. PHYSICAL MODEL

2.1 Description of the Proposed System

The solar cooker proposed in this study is composed of a solar concentrator and a parallelepiped enclosure, where the pot containing the food to be cooked is placed. The pot is a semi-spherical tank with a black painted outer wall. The walls of the parallelepiped enclosure, with the exception of the wall facing the concentrator, are made of wood measuring $0.65\text{ m} \times 0.50\text{ m} \times 0.50\text{ m}$, and glass wool is used for insulation. In front of the device is a window through which the solar flux reflected by the concentrator is transmitted. Access to the interior of the enclosure is through one of the vertical walls adjacent to the glass wall, designed as a door.

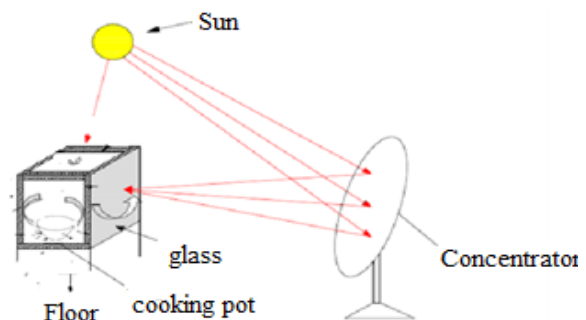


Fig. 1. Synoptic diagram of the cooker

The figure below shows the cooking box containing the kettle in the form of a semi-spherical tank. In this box we show the different phenomena of heat transfer.

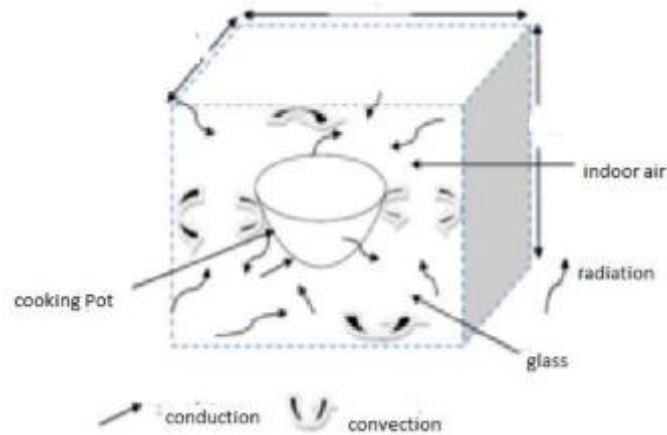


Fig. 2. Block diagram of the firing box and the physical phenomena occurring in it

3. EQUATION OF TRANSFER

The application of Ohm's law to the electrical analogue given by equation (Eq1) leads to the system of equations of heat and mass exchange coefficients

$$M_i C_{pi} \frac{\partial T_i}{\partial t} = \varphi_{sol} \times S_i + \sum_{k=1}^m \sum_{j=1}^n (h_{r,j-k} + h_{cv,j-k} + h_{cond,j-k})(T_k - T_j)$$

On both sides of the glass we have heat transfer by radiation and natural convection with the environment, and heat transfer by conduction through the facades

$$m_v C_p \frac{\partial T_{ve}}{\partial t} = I \alpha_v S_v + h_{rv} S_v (T_{ciel} - T_{ve}) + h_{rvsol} S_v (T_{sol} - T_{ve}) + h_{cv} S_v (T_{amb} - T_{ve}) + \frac{\lambda_v S_v}{e} (T_{vi} - T_{ve})$$

$$m_v C_p \frac{\partial T_{vi}}{\partial t} = I \alpha_v S_v + h_{rmv} S_m (T_{pme} - T_{vi}) + h_{cvv} S_v T_{ai} - T_{vi} + \lambda_v S_v e v T_{ve} - T_{vi}$$

Inside the enclosure, the speed of air movement is low, the heat transfer is by convection between the glass and the air and then between the glass and the wall of the pot.

$$m_{ai} C_{pai} \frac{\partial T_{ai}}{\partial t} + m_{ai} C_{pai} V_{ai} \frac{\partial T_{ai}}{\partial x} = h_{cvai} S_v (T_{vi} - T_{ai}) + h_{cvm} S_m T_{pme} - T_{ai}$$

In this equation, we will neglect the term $\frac{\partial T_{ai}}{\partial x}$ in front of the term $\frac{\partial T_{ai}}{\partial t}$ indeed as the speed of displacement is very weak, we consider that the variation of temperature in a given point due to

the exchanges with the various mediums present is considerable in front of the variation of temperature due to the displacement of the air.

The pot is considered as an absorber, it has two faces: external and internal. We write the differential equations on each side where the heat transfer is done by convection, radiation and conduction.

$$m_m C_{pm} \frac{\partial T_{pme}}{\partial t} = I \tau_v \alpha_m + h_{cvm} S_m (T_{ai} - T_{pme}) + h_r S_m T_{vi} - T_{pme} + 2\pi \lambda_m R_2 - R_1 R_2 \cdot R_1 T_{pme} - T_{pme}$$

$$m_m C_{pm} \frac{\partial T_{pmi}}{\partial t} = 2\pi \lambda_m \left(\frac{R_2 - R_1}{R_2 \cdot R_1} \right) (T_{pme} - T_{pmi}) + h_f S_m (T_f - T_{pmi})$$

Equation (7) justifies the evolution of the temperature of the fluid in the kettle

$$m_f C_{pf} \frac{\partial T_f}{\partial t} + m_f C_{pf} V_f \frac{\partial T_f}{\partial x} = h_f S_m (T_{pmi} - T_f)$$

Heat is exchanged by the three modes of heat transfer: conduction, convection and radiation.

4. METHODOLOGY

The method of resolution is the Gaussian method coupled with an iterative procedure because of the convective and radiative heat transfer coefficients which depend on the unknown temperatures of the different media. Thus, in this case, the calculations are incremented by one time step and this procedure is continued over

time until the desired accuracy and running time of the solar cooker is reached.

5. RESULTS AND DISCUSSION

5.1 Numerical Code Validation

In order to validate our numerical code, we applied it to the model treated numerically and experimentally by Soria [40]. The cooker built by Soria is a box type with wooden walls of dimensions 0.22x0.52x0.70 m consisting of a double glazing in front of the solar concentrator. The walls are insulated with 2cm thick cork sheets placed on their inner sides. This comparison shows a perfect agreement (qualitative and quantitative) between our numerical results and those obtained from Soria, with regard to the correlation coefficient $R^2=0.9020$ and the maximum relative deviation obtained, of the order of 2%.

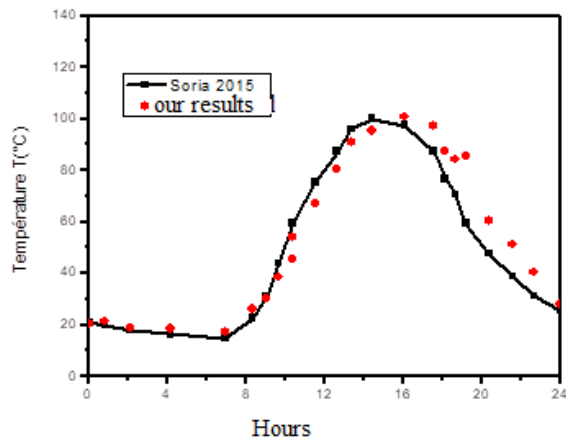


Fig. 3. Hourly temperature variation of the air inside the cooking box

6. ANALYSIS OF PHYSICAL PARAMETERS

The figures below illustrate the evolution of the influence of the different parameters of the cooker. These figures show that the parameters are a function of the materials covering the surface of the concentrator.

6.1 Influence of the Nature of the Concentrator Coating Materials

In this section we present the influence of the nature of two materials of the concentrator lining whose properties are shown in the Table 1.

Table 1. Radiative coefficients of concentrator materials

Materials	Reflectivity	Emissivity
Aluminium foil	0,65	0,09
Mirror	0,99	0,97

Figs. 4-5 show the evolution of the temperature at the focus of the concentrator as a function of solar irradiance. As shown in Figs. 4 and 5, the temperature at the focus of the concentrator with rectangular mirrors on the wall is higher than that of the concentrator with aluminium foil on the wall. Thus, for an opening diameter of 65 cm, the temperature at the focus of the concentrator covered with rectangular mirrors is 160°C and the thermal efficiency is 80%. For a solar irradiance equal to 900W/m² and an opening diameter of the concentrator of 65 cm, the temperature at the focus of the concentrator covered with aluminium film reaches 118°C with a thermal efficiency of 60%. From these results,

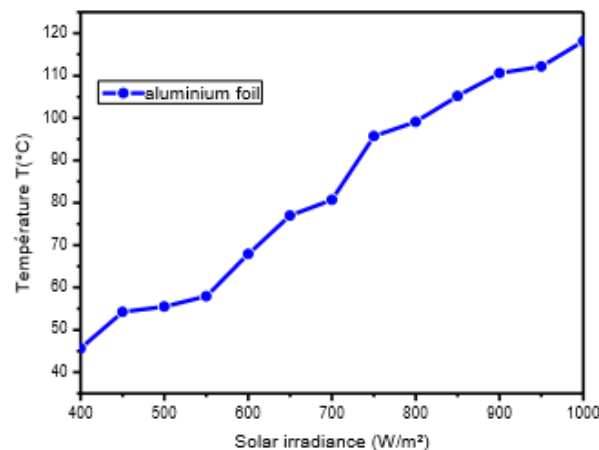


Fig. 4. Evolution of the temperature at the focus of the concentrator as a function of solar irradiance. Concentrator wall covered with aluminium foil

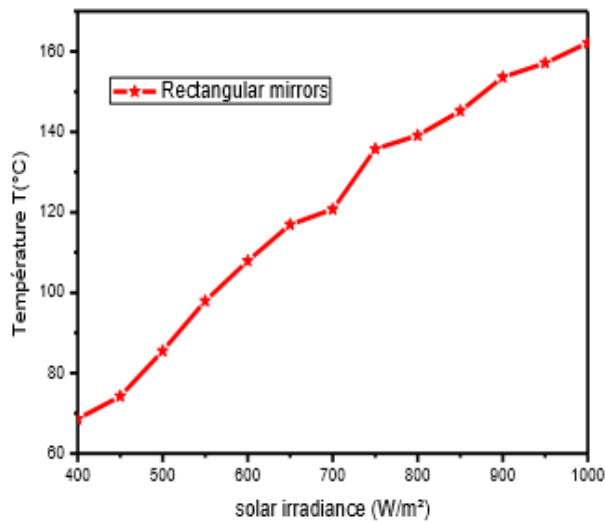


Fig. 5. Evolution of the temperature at the focus of the concentrator as a function of solar irradiance. Concentrator wall covered with rectangular mirrors

we retain the concentrator with rectangular mirrors on the wall for further calculations. This confirms the superior optical properties of the mirror as shown in Table 1.

7. INFLUENCE OF THE DIMENSIONS OF THE COOKER

In this paragraph, we look for the optimal dimensions of the cooker, more precisely the values of the length, height and width of the parallelepipedic enclosure in which the kettle is placed, for which the air temperature reached is maximum under the operating conditions retained previously.

The various figures below show the evolution of the air temperature inside the

chamber as a function of the dimensions of the cooker.

Note that in Fig. 6, the air temperature decreases as the length of the cooker enclosure increases. Figs. 7 and 8 illustrate that the air temperature in the cooker chamber increases as the other dimensions (height, width) increase.

In order to define the optimal dimensions of this cooker, Fig. 6 illustrates the evolution of the temperature in the cooker chamber as a function of its dimensions (length, width and height). We notice that the optimal dimensions are located in the ABC zone where the temperature is maximum. Therefore, the optimal height and width are 0.50 m and the optimal length is 0.65 m.

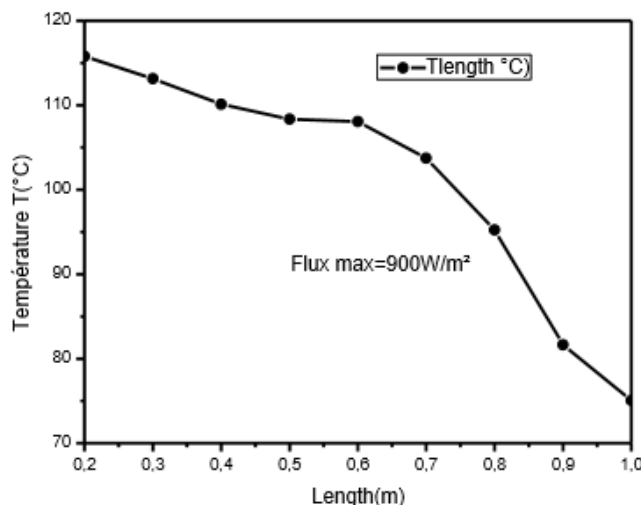


Fig. 6. Evolution of the air temperature in the cooker chamber as a function of width

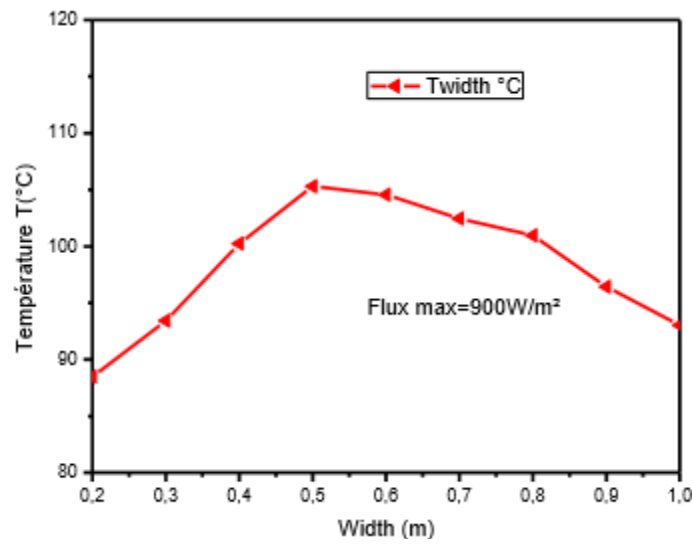


Fig. 7. Evolution of the air temperature in the cooker chamber as a function of width

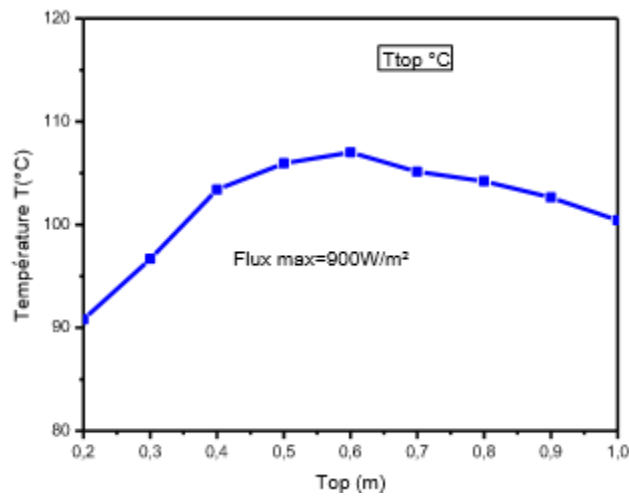


Fig. 8. Evolution of the air temperature in the cooker chamber as a function of height

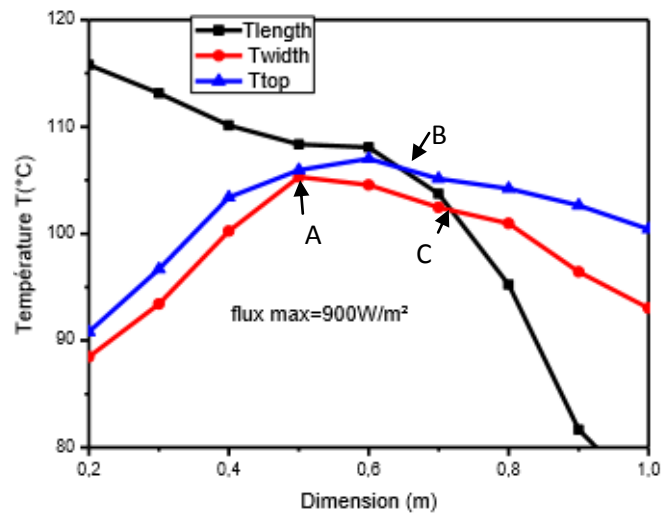


Fig. 9. Evolution of the air temperature in the cooker chamber as a function of its dimensions

The result shows that for dimensions between [50 cm-65 cm], the thermal efficiency of the cooker is in the range of 42-45%. Thus, for a solar flux reflected by the concentrator, the higher the temperature rise of the fluid in the pot, the smaller its volume. From this curve, we deduce that the dimensions 0.65x0.50x0.50 m for which the energy yield reaches its maximum value are the optimal dimensions of the cooker. In the rest of our calculations, we will use these dimensions.

8. INFLUENCE OF THE DIFFERENT MATERIALS OF THE POT WALLS

Fig. 10 shows the hourly evolution of the temperature of the external face of the kettle. We analyse the influence of the nature of the materials it is made of.

The values of the thermo-physical properties of these materials are given in Table 2.

The nature of the materials of which the kettle is made plays a very important role in the value of the temperature of the fluid it contains.

We observe that the hourly changes in the highest temperature of the fluid it contains are

similar throughout the day. However, the highest values are obtained for the pot with a copper wall, the material with the highest thermal conductivity among those used in our calculations.

The analysis of the influence of the thickness of the pot wall shows that the lower the thickness of the pot, the higher the temperature of the inner side of the pot (Fig. 10).

The nature of the materials of which the kettle is made plays a very important role in the value of the temperature of the fluid it contains.

We observe that the highest hourly temperature changes of the fluid contained in it are similar during the day. However, the highest values are obtained for the pot with a copper wall, which is the material with the highest thermal conductivity.

9. INFLUENCE OF THE THICKNESS OF THE POT WALLS

The analysis of the influence of the thickness of the pot wall shows that the lower the thickness of the pot, the higher the temperature of the inner side of the pot (Fig. 11).

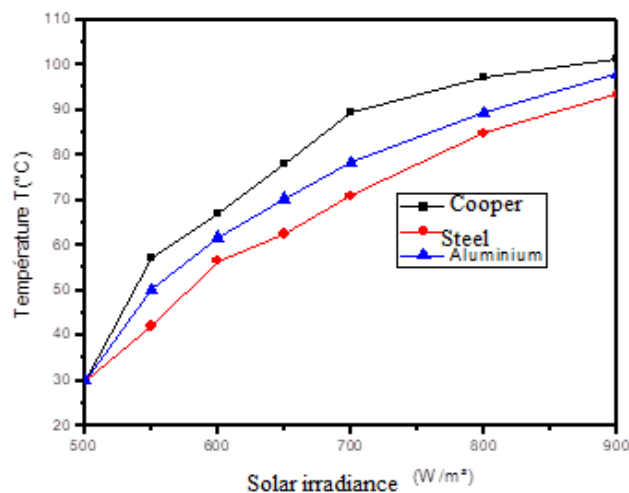


Fig. 10. Hourly temperature trends on the outer surface of the wall showing the influence of the nature of the material constituting the wall of the kettle

Table 2. Thermo-physical properties of the materials of which the pot wall is made

Materials	Thermal conductivity (W/m.K)	Specific heat (J/kg.K)	Density Kg/m ³
Aluminium	237	896	2700
Steel	50	450	7800
Copper	401	386	8940

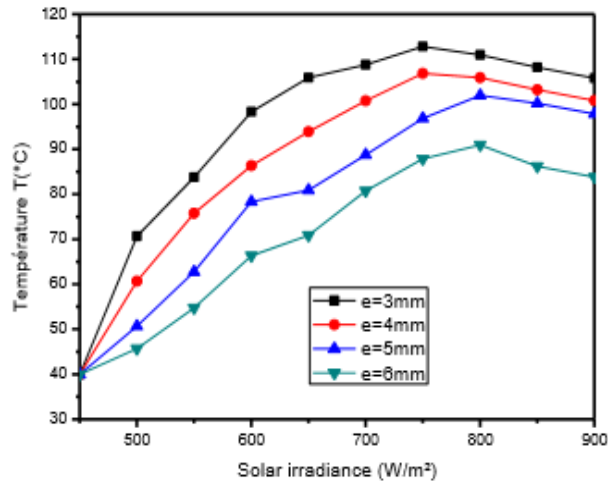


Fig. 11. Hourly temperature trend of the outer side of the pot wall for different pot thicknesses

Table 3. Values of thermal efficiency and heat exchange coefficient

Wall thickness	Thermal efficiency %
e=3 mm	61,38
e=4 mm	58,40
e=5 mm	44,62
e=6 mm	36,91

This result is consistent with the fact that the thermal resistance between the outer and inner surfaces is greater the greater the thickness of the wall. The wall thickness is of the order of a few millimetres. Thus, the thermal efficiency by conduction through the wall of the kettle becomes important when the thickness is low. This result is consistent with the hourly temperature evolution of the fluid in the kettle.

10. CONCLUSION

In this work, a numerical study of the solar cooker was carried out.

A model of the heat transfers in this cooker was then proposed. The equations governing the heat transfers are obtained from heat balances established on each component of the cooker and based on the nodal method. These equations are discretised by the implicit finite difference method, coupled with an iterative Gaussian algorithm procedure.

The simulation shows that the thermal resistance is low when the thermal conductivity is higher. It is clear that the physical parameters of the cooker play a major role in determining the dimensions of the cooker. In addition, the increase in the temperature of the pot wall helps

to improve the thermal efficiency of the solar cooker studied.

ACKNOWLEDGEMENT

The author would like to thank all the contributors who have contributed in various ways, for providing the financial the necessary facilities and constant encouragement for the present study.

COMPETING INTERESTS

Authors have declared that no competing interests exist.

REFERENCES

- Gama A. Etude et réalisation d'un concentrateur cylindro parabolique avec poursuite solaire aveugle Revue des Energies Renouvelables. 2008;11(3):437–451.
- Boukhchana Y. Theoretical and experimental study of a cylindro-parabolic solar collector. Journal of Environmental Science and Engineering. 2011;5:1026–1030.
- Yasmina Boukhchana. Etudes théorique et expérimentale des performances d'un

- capteur solaire cylindro- parabolique, (5^e Congrès International Energie Renouvelable et Environnement).
4. Sharaf E. A new design for an economical, efficient, conical solar Cooker. *Renewable Energy*. 2002;27:599-619.
 5. Yacine Marif. Étude comparative entre les modes de poursuite solaire d'un concentrateur solaire cylindro-parabolique, *Annales Des Sciences et Technologies*. 2014;6(2).
 6. Mokhtar G. Simulation Numérique d'un Concentrateur Cylindro-Parabolique en El Oued, Algérie. *International Journal of Scientific Research & Engineering Technology (IJSET)*. Copyright IPCO-2015;3(2):68-74. ISSN: 2356-5608.
 7. Al-Soud M S. A parabolic solar cooker with automatic two axes sun tracking system, *Applied Energy*. 2010;87:463–470.
 8. Klemens Schwarzer. Characterisation and design methods of solar cookers, *Solar E Mgmtvol*. 1990;30(1):9-16.
 9. José M. Arenas, Design, development and testing of a portable parabolic 2. *Solar Kitchen*; march 2006.
 10. Judith. Multiple use communal solar cookers. *Solar Energy*. 2004;77:217–223.
 11. Pohekar SD. Utility assessment of parabolic solar cooker as a domestic cooking device in India. *Renewable Energy*. 2006;31:1827–1838.
 12. Fraser P. Stirling dish system performance and prediction model. MSc thesis in mechanical engineering. Madison, USA: University of Wisconsin; 2008.
 13. Rabl A. Solar concentrators with maximal concentration for cylindrical absorbers. *Applied Optics*. 1976;15(7):1871–3.
 14. Mohamed, Parabolic solar cooker with automatic system tracking two axis. *Applied Energy*. 2010;87:463-470.
 15. Kumar S, Reddy N. Numerical investigation of natural convection heat loss in modified cavity receiver for fuzzy focal solar dish concentrator. *J Solar Energy*. 2007;81: 846–55.
 16. Ali A. Portable solar cooker and water heater, *Energy Conversion and Management*. 2010;51:1605-1609.
 17. Mullick. Thermal test procedure for a paraboloid concentrateur solar cooker. *Solar Energy*. 1991;46(3):39-144.
 18. Kumar S, Reddy N. Numerical investigation of natural convection heat loss in modified cavity receiver for fuzzy focal solar dish concentrator. *J Solar Energy*. 2007;81: 846–55.
 19. Rabl A. Solar concentrators with maximal concentration for cylindrical absorbers. *Applied Optics*. 1976;15(7): 1871–3.
 20. Judith Franco, Pasteurization of goat milk using a low cost solar concentrator, *Solar Energy*. 2008;82:1088-1094.
 21. Patel NV, Philip SK. Performance evaluation of three solar concentrating cookers. *Renewable Energy*. 2000;20: 347–55.
 22. Rachel. Development and performance analysis of compound parabolic solar concentrators with reduced gap losses— 'V' groove reflector. *Renewable Energy*. 2002;27:259–275.
 23. Severin Campuzano. Development of the solar cooker jorhejpatarnskua: Thermal standard analysis of solar cooker with several absorber pots. *Energy Procedia*. 2014;57:1573–1582.
 24. Sonune AV. Development of a domestic concentrating cooker, *Renewable Energy*. 2003;28:1225-134.
 25. Abu-Malouh R. Design, construction and operation of spherical solar cooker with automatic sun tracking system, *Energy Conversion and Management*. 2011;52: 615–620.
 26. Funk P. Evaluating the international standard procedure for testing solar cookers and reporting performances, *Solar Energy*. 2000;68(1):1-7.
 27. Olwi A. Computer simulation of the solar pressure cooker. *Solar Energy*. 1988; 40(3):259–268.
 28. Peajack ER. Mathematical model of the thermal performance of box-type solar cookers. *Renewable Energy*. 1991;1(5/6): 609–615.
 29. Soriaverdugo. Experimental analysis and simulation of the performance of a box-type solar cooker, *Energy for Sustainable Development*. 2015;29:65–71.
 30. El-Sebaili AA. Thermal performance of a box type solar cooker with outer-inner reflectors. *Energy*. 1997;22:969–78.
 31. Kawthar Dhif. Thermal Analysis of the Solar Collector Cum Storage System Using a Hybrid-Nanofluids. *Journal of Nanofluids*. 2021;10:616–626.
 32. Ines Chabani. MHD Flow of a Hybrid Nano-Fluid in a Triangular Enclosure with

- Zigzags and an Elliptic Obstacle, Academic Editors; January 2022
33. Mehemet Esen. Thermal performance of a solar cooker integrated vacuum- tube with heat pipes containing different refrigerants; December 2003.
 34. Sharma. Thermal performance evaluation of a latent heat storage unit for late evening cooking in a solar cooker having three reflectors; April 2002.
 35. Olwi. Towards convenient solar cooking experimental results of an indoor model, Energy Convers Mgmt. 1994;35(9):793-799.
 36. Hussein. Experimental investigation of novel indirect solar cooker with indoor PCM thermal storage and cooking unit, Energy Conversion and Management. 2008;49:2237–2246.
 37. Abishek. A thermodynamic review on solar box type cookers, Renewable and Sustainable Energy Reviews. 2011;15: 3301–3318.
 38. Morakapala. Domestic solar hot water systems: Developments, evaluations and essentials forviability with a special reference to India. Renewable and Sustainable Energy Reviews. 2011;15: 3850–3861.
 39. Daniel M Kammen. Comparative study of Box-type Solar Cooker in Nicaragua. Solar & Wind Technology. 1990;7(3):463-471.
 40. Soria Verdugo. Experimental analysis and simulation of the performance of a box-type solar cooker. Energy for Sustainable Development. 2015;29:65–71.

ANNEX

Through the pane of thickness e_v and thermal conductivity λ_v the conductive transfer coefficient is by definition equal to:

Conductive Heat Exchange

The coefficient of heat transfer by conduction through the wall of the pot, h_{cp} assimilated to a half-sphere, verifies the following expression:

$$h_{cpm} = \frac{2 \times \pi \times \lambda_m \times (R_2 - R_1)}{S_m \times R_2 \times R_1}$$

By Convection

Between the external face of the glass and the ambient air

$$h_{cv-a} = 5,67 + 3,86V_v$$

Between the inner face of the glass and the air inside the parallelepiped enclosure

$$h_{cvvai} = \frac{\lambda_v \times N_{ust}}{H_v}$$

Between the outside of the absorber wall and the air inside

$$h_{cvpmai} = \frac{\lambda_m \times N_{us}}{H_m}$$

Between the fluid and the inside of the absorber wall

$$h_{cvpmf} = \frac{\lambda_f \times N_{us}}{H_m}$$

By Radiation

Between the outer face of the glass and the sky

$$h_{rciel} = [\sigma \cdot S (T_{ve}^2 + T_{ciel}^2) (T_{ve} + T_{ciel})] \times \frac{(1 + \cos \alpha)}{2}$$

Where α is the angle of inclination of the pane to the horizontal.

Between the outer face of the pane and the ground

$$h_{rsol} = [\sigma \cdot S (T_{ve}^2 + T_{sol}^2) (T_{ve} + T_{sol})] \times \frac{(1 - \cos \alpha)}{2}$$

Between the absorber and the inside of the glass

$$h_{rv-m} = \frac{\sigma (T_{vi} + T_{pme}) (T_{vi}^2 + T_{pme}^2)}{\frac{1}{\epsilon_{rvm}} + \frac{1}{\epsilon_m} + \frac{1}{\epsilon_v} - 1}$$

The Nusselt number has the expression:

$$N_{us} = \left[0,825 + \frac{0,387 \times R_a^{\frac{1}{4}}}{\left[1 + \left(\frac{0,492}{Pr} \right)^{\frac{1}{4}} \right]^{\frac{1}{2}}} \right]^2$$

$$3.10^5 < R_a < 3.10^{10}$$

$$N_{ust} = 0,27 \times R_a^{\frac{1}{4}}$$

The number of Grashof

$$G_r = \frac{g\beta\Delta T_p^2 L^3}{\mu^2}$$

The Rayleigh number

$$R_a = \frac{g\beta(T_p - T_\infty)L^3}{\alpha\nu^2}$$

The sky temperature is deduced by the correlation of:

$$T_{ciel} = 0,0552T_a^{1,5}$$

The room temperature is calculated using the expression:

$$T_a = \bar{T}_a + \Delta T_a \times \sin\left\{\frac{\pi}{12} \times [TL - (TLo + \frac{3}{2})]\right\}$$

TL: Local time (h)

TLo: Sunrise time (h)

$$\bar{T}_a = \frac{T_{a,max} + T_{a,min}}{2} \quad \text{et} \quad \Delta T_a = \frac{T_{a,max} - T_{a,min}}{2}$$

© 2023 Gbembongo et al.; This is an Open Access article distributed under the terms of the Creative Commons Attribution License (<http://creativecommons.org/licenses/by/4.0>), which permits unrestricted use, distribution, and reproduction in any medium, provided the original work is properly cited.

Peer-review history:

The peer review history for this paper can be accessed here:

<https://www.sdiarticle5.com/review-history/90958>